

Electrolyte gated TFT biosensors based on the Donnan's capacitance of anchored biomolecules

Kyriaki Manoli^a, Gerardo Palazzo^{*a,b}, Eleonora Macchia^a, Amber Tiwari^a, Cinzia Di Franco^c, Gaetano Scamarcio^{c,d}, Pietro Favia^e, Antonia Mallardi^f and Luisa Torsi^{a,b}

^aDipartimento di Chimica, Università degli Studi di Bari "A. Moro", Via Orabona 4, 70125, Bari

^bCSGI (Center for Colloid and Surface Science) Bari

^cCNR - Istituto di Fotonica e Nanotecnologie, Sede di Bari

^dDipartimento di Fisica "M. Merlin", Università degli Studi di Bari "A. Moro", Via Orabona 4, 70125, Bari

^eDipartimento di Bioscienze, Biotecnologie e Biofarmaceutica, Università degli Studi di Bari "A. Moro", Via Orabona 4, 70125, Bari

^fCNR-IPCF, Istituto per i processi chimico fisici, c/o Dip. Chimica, via Orabona 4, 70125, Bari

ABSTRACT

Biodetection using electrolyte gated field effect transistors has been mainly correlated to charge modulated transduction. Therefore, such platforms are designed and studied for limited applications involving relatively small charged species and much care is taken in the operating conditions particularly pH and salt concentration (ionic strength). However, there are several reports suggesting that the device conductance can also be very sensitive towards variations in the capacitance coupling. Understanding the sensing mechanism is important for further exploitation of these promising sensors in broader range of applications. In this paper, we present a thorough and in depth study of a multilayer protein system coupled to an electrolyte gated transistor. It is demonstrated that detection associated to a binding event taking place at a distance of 30 nm far from the organic semiconductor-electrolyte interface is possible and the device conductance is dominated by Donnan's capacitance of anchored biomolecules.

Keywords: biosensor, electrolyte gated thin film transistors, gate capacitance, Donnan's equilibrium

1. INTRODUCTION

Electrolyte gated thin film transistors (EG-TFTs) technology has demonstrated ultra-sensitive, low cost and label free biosensors^{1,2}. Indeed, while organic semiconductor based transistor sensors have been gathering attention since decades³, electrolyte-gated organic field-effect transistors are a relatively new class of sensors based on an electronic principle of transduction. EG-TFT structure employs an organic semiconductor (OS) that connects the source and drain electrodes, forming the active channel. Typically, the top surface of the semiconductor is in ionic contact with a gate electrode via an electrolyte. The ionically conducting and electronically insulating electrolyte acts as the gate dielectric in conventional TFTs. In this case a fully insulating medium is used. Upon application of a potential to the gate electrode, electric double layers (EDLs) are formed at the semiconductor/ electrolyte and the electrolyte/ gate interfaces^{4,5}. The amount of charges induced at the interface of semiconductor with the electrolyte and consequently the conductivity of the semiconducting channel is controlled by the gate voltage. Among the most common approaches to incorporate the sensing element in the EG-TFT structure is by anchoring specific receptors on the surface of the active channel. Therefore, the semiconductor surface is functionalized with biorecognition molecules capable of recognizing and capturing a specific target analyte⁶⁻⁸. Upon binding, charges on the captured molecules modify the OS's surface potential. This change in the electrical field causes accumulation or depletion of carriers in the semiconductor channel, resulting in an augment or reduction of the drain current.

When an electrolyte such as a buffer solution (*i.e.* phosphate buffered saline, PBS) is used as gating medium, the dissolved charged species form, at the interface solid/solution, electrical double layers that are known screen the charge of the biomolecules. This effect is an important parameter, impacting on the TFT's sensing performance. The ion-induced electric field screening has an exponential-like behavior and beyond a certain distance, that is the Debye length (λ), the transistor becomes insensitive to detect variations due to electrostatic effects. A short Debye length is

expected to screen most of the charges when using a high ionic strength (i_s) buffer solution. For instance, in a 1x PBS to 0.1x PBS, λ goes approximately from 0.7 to 2.2 nm, respectively. Several studies have shown that for distances from the surface as short as 2 nm, the detection of small molecules such as DNA is possible⁹. However, for larger sized proteins, such as antibodies, TFT detection of charged molecules is negatively affected by ion screening. Few years back the pioneering works of Stern *et. al.* demonstrated the effect of Debye screening length on a nanowire (NW) based TFT biosensing platforms^{10, 11}. Primarily, biotin- avidin model system was investigated. In a following up work, an antibody- antigen system was also explored. It was shown that the signal of the response upon ligand binding increases as we go from high to lower salt concentrations of the electrolyte solution. On the other hand, it has been demonstrated that EG-TFTs can sense binding events far from the channel namely, at distances much larger than the λ ¹². This clearly indicates that the EG-TFT detection is not solely based on the electrostatic perturbation that the analyte charge induces on the semiconductor. Therefore, other phenomena can be associated to the transduction mechanism. Important to outline is also that label-free detection of large charged and neutral species has been also reported, where the sensing mechanism was correlated with capacitance induced changes^{13, 14}.

In order to identify the origin of capacitance modulated transduction in EG-TFTs, it is necessary to describe in detail all the components of the gate capacitance. As mentioned, in the case of electrolyte gated transistors, upon gate biasing EDLs form at each interface of the electrolyte medium. Consequently, the total capacitance (C_{TOT}) of the gate-electrolyte-semiconductor system is given by the series of the gate-electrolyte capacitance (C_{GE}) and electrolyte-semiconductor capacitance (C_{ES}). If the two EDL capacitances are equal ($C_{GE} = C_{ES} = C$), the total capacitance is C_{TOT} is equal to $C/2$, otherwise the smallest capacitance will dominate. Each EDL can be further described by the Stern model. According to that, within the electrolyte the ion layer is composed of two layers, the Helmholtz double layer (HDL) and the diffusion layer. All the applied voltage is dropped across the two HDL generating large capacitances ($> 10 \mu\text{F}/\text{cm}^2$). This is true for high ions concentration solution, like ionic liquids and solid polyelectrolytes. The situation changes when conventional buffer solutions are employed as gating medium. In such a case, only a small fraction of charges is located in the HDL, while the rest form the Gouy-Chapman diffuse double layer (GCDL). Thus, the overall capacitance of each EDL can be described as a series connection of the HDL and GCDL capacitance and will be governed by the smallest one. This implies that the sensitivity of the EG-TFT can be easily enhanced by the proper design of the transistor based sensors. For example, if bioreceptors are integrated on the surface of the OS, the biorecognition event may result in a variation of the gate capacitance and hence the maximum sensitivity is achieved when $C_{ES} \ll C_{GE}$. The gate capacitance can indeed be reduced due to low permittivity of adsorbed biomolecules relative to the electrolyte¹⁵. Theoretical studies have shown that electrostatic capacitance changes due to adsorbed biomolecules are significant in case of almost full coverage and when ions from the electrolyte cannot penetrate through the protein layer¹⁶.

Herein, to demonstrate how the EG-TFT response differs upon electrostatic and capacitance effects, we studied a three-protein multilayer system. A bio EG-TFT sensing platform comprising a biological layer at the interface between the OS and the electrolyte was used (Figure 1). The biological layer was composed of a biotinylated phospholipid (PL) bilayer covalently attached to the OS surface through a plasma-deposited ultrathin coating film providing $-\text{COOH}$ moieties (system A). Biotin served to selectively bind streptavidin (SA) and/or avidin (AV). The SA(AV)/PL layer resulted in a new bio-receptor layer (*system B*). The remaining binding sites of tetrameric SA(AV) were further exposed to biotinylated anti-body (aB) leading to the *system C*. The latter was used to detect C-reactive protein (CRP) Binding of CRP to the system C give rise to the three-proteins multilayers *system D*. Summarizing, the obtained protein arrangements result in binding events occurring at different distances from the channel, 5 nm (binding of AV to *system A*), 15 nm (binding of aB to *system B*), 25 nm (CRP binding to *system C*). This allowed discriminating between charge and capacitance modulated transduction.

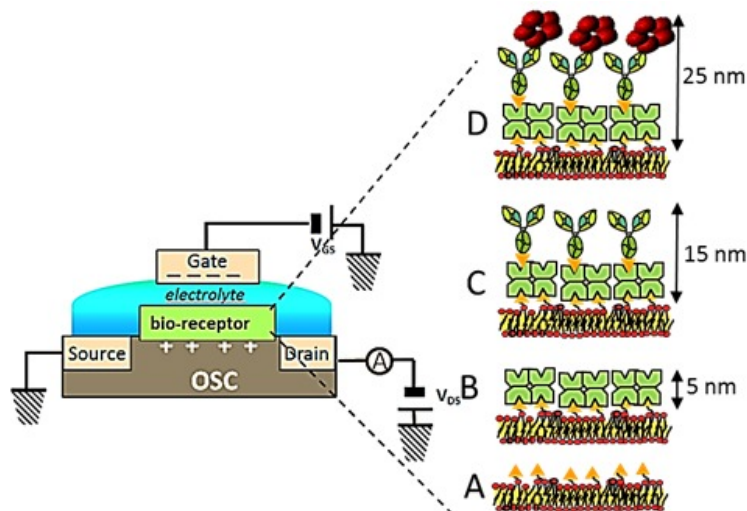


Figure 1. Schematic structure of the EG-TFT device with the different protein multilayer stack

2. MATERIALS AND METHODS

2.1 Materials

Poly-3hexylthiophene (P3HT regioregular > 98%) was purchased from Rieke Metals and used after purification by successive Soxhlet extractions with methanol and hexane as reported previously¹⁷. Indeed, thiophene based organic semiconductors are known for being characterized by a polycrystalline morphology, suitable for sensing applications^{18, 19}. Soy bean lecithin (EPIKURON 200) and N-((6 (Biotinoyl)amino)hexanoyl)-1,2-Dihexadecanoyl-sn-Glycero-3-Phosphoethanolamine (Biotin-X DHPE) were respectively purchased from Cargill and Invitrogen. Streptavidin from *Streptomyces avidinii*, Avidin from egg white and all the other chemicals and solvents were obtained by Sigma-Aldrich. The biotinylated Anti-CRP monoclonal antibody (Ab) and the CRP protein from human plasma were respectively purchased from HyTest and Scripps Laboratories.

2.2 EG-TFT biosensor fabrication

Device fabrication

Si/SiO₂ substrates with interdigitated gold source (S) and drain (D) electrodes (10 μm channel length and 10 nm channel width) were obtained by photolithographically defining the S and D electrodes using vacuum-deposited titanium as gold adhesion-promoter layer. The substrates were first cleaned using solvents of increasing polarity, then a purified P3HT chloroform solution (2.6 mg mL⁻¹) was spin-coated on the bottom-contact devices and subsequently annealed at 75 °C for 1h.

Biofunctionalization fabrication protocol

Plasma –treatment: P3HT surface was first functionalized with a plasma-deposited thin layer characterized by a certain surface density of -COOH moieties, as confirmed by X-ray Photoelectron Spectroscopy. The same deposition protocol reported previously was used²⁰. Plasma depositions were carried out in a home-build low pressure RF (13.56 MHz) plasma reactor described elsewhere²¹. Acrylic acid vapors (AA>99%, Aldrich, USA), ethylene (Eth, Air Liquide) and argon (Ar, Air Liquide) were used in mixture as feed. The following deposition conditions were used: power 50 W, pressure 250 mTorr, flow rates: $\Phi_{AA} = 2.5$ sccm, $\Phi_{Eth} = 7.5$ sccm, $\Phi_{Ar} = 2.5$ sccm. A deposition time of 3s was used, corresponding to coatings with a nominal thickness of 1.7 nm. The static water contact angle of the -COOH functionalized P3HT layer was lowered from $104 \pm 4^\circ$ to $80 \pm 1^\circ$ in this way. Plasma deposition conditions were optimized to the best stability of the -COOH functionalized coatings in water media²².

Vesicles preparation and covalent attachment: 4.5 mg of soybean lecithin, 0.5 mg of phosphatidylethanolamine and the proper amount (50-150 μg) of biotin-X DHPE were dissolved in chloroform. The solvent was then evaporated

under N₂ flow and the phospholipids were kept 60 min under vacuum. Phospholipids were rehydrated in 1 mL PBS and sonicated 10 min on ice. The obtained multilamellar vesicles suspension was repeatedly extruded through a polycarbonate filter with 100 nm pore sizes using the Avanti mini-extruder (Avanti Polar), to obtain single unilamellar vesicles.

PL vesicles were immobilized onto plasma-modified EGOFETs through the formation of amidic bonds between the -COOH surface groups and the NH₂ moieties on the polar heads of phosphatidylethanolamine. The EGOFETs were incubated in a freshly prepared EDC/S-NHS (both 100 mM in PBS) solution for 1 h at room temperature. After the EDC/S-NHS treatment, samples were rinsed in PBS three times and incubated over-night under mild agitation in the vesicles suspension at room temperature. Specimens were finally extensively washed in PBS. The static water contact angle was lowered from 80±1 to 23±5°.

Deposition of the proteins: The PL/SA(AV) multilayer was prepared by adding to the PL bilayer (according to the above procedure) a SA (AV) solution at 100 µg/mL for 15 min and extensively rinsing with buffer. The subsequent protein layers were prepared by adding in the biotinylated anti-CRP solution (PL/SA(AV)/Ab) and the CRP solution (PL/SA(AV)/Ab/CRP), both at 100 µg/mL. After each step the surface was rinsed thoroughly with PBS.

2.3 Electrical and sensing measurements

The electrical measurements were performed by recording the transfer characteristics (I_{DS} vs. V_G at $V_{DS} = -0.5$ V) of the EG-TFT devices using a Keithley 4200-SCS semiconductor parameter analyzer. A gold plate (1x1 mm²) in contact with a droplet (2 µL) of PBS ($i_s = 0.163$ M, 10 mM, KCl 2.7 mM, 137 mM NaCl, pH = 7.4) was used as gate electrode and the measurements were performed in a water vapour saturated chamber. The transistor electrical figures of merit, namely the field-effect mobility (μ), the threshold voltage (V_T) and on/off current ratio, were extracted from the transfer characteristics in the saturation regime²³. SA (AV) sensing measurements were carried out by exposing the PL modified active channel for 15 minutes to the protein solution. The channel was then rinsed three times with buffer, to remove the unbound proteins and finally the response was evaluated as the I_{DS} relative current variation at $V_G = -0.5$ V with respect to PBS. The response-dose curve was obtained by measuring solutions of increasing protein concentration on the same device. The data shown are the average and the standard deviation of measurements replicated on at least three different EG-TFT channels. The same procedure was followed for the rest of the protein layers (anti-CRP and CRP).

2.4 Proteins dimension and charge

Avidin and Streptavidin²⁴ hold similar size (~ 5nm) but differ in the isoelectric point²⁵, so that at pH=7.4 the SA is negatively and the AV is positively charged. The antibody against the C-reactive protein was characterized for its size and charge using an electrophoretic dynamic light scattering apparatus (Zetsasizer ZS-nano by Malvern). The measurements in PBS at pH=7.4 gave a hydrodynamic diameter of 15±1 nm and a negative charge (Z-potential = -9.3±0.7 mV). The C-reactive proteins (CRP) is a pentameric protein with a diameter of about 11 nm²⁶. It was characterized for its size and charge as well. In PBS at pH=7.4, CRP was found to have a hydrodynamic diameter of 9.5±0.2 nm and a negative charge (Z-potential = -6.8±0.6 mV).

3. RESULTS AND DISCUSSION

In figure 2, the transfer characteristics for the proteins multilayers based on SA and AV are shown. Upon SA and AV binding to system A (plain PL bilayer), the device behaves differently. The binding of these proteins to the PL bilayer has an opposite effect on the output current; SA increases the drain current (figure 2a) whereas AV causes a significant decrease (figure 2b). On the other hand, the addition of the aB layer (system C) is seen as a decrease of the current for both SA and AV. Interestingly, CRP loading to the surface (system D) gave rise to the drain current. The experimental data suggest that in the case of SA and AV the response of the EG-TFT depends on the protein properties while for ab and CRP the signal are independent on the protein nature. Moreover, it seems that the binding of proteins to the outermost bio-layer influences the I-V transfer characteristics although the distance from the channel is far beyond the Debye length.

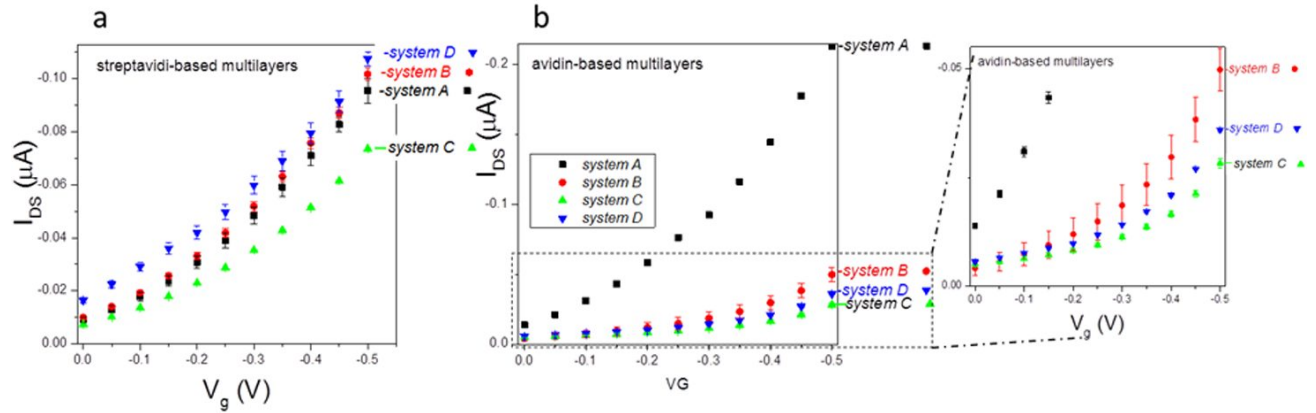


Figure 2. Transfer characteristics for: a) PL (system A), PL/SA (system A), PL/SA/Ab (system B), PL/SA/Ab/CRP(system D) and b) PL (system A), PL/AV (system A), PL/AV/Ab (system B), PL/AV/Ab/CRP(system D).

Cumulative response-dose curves for the binding of SA, AV, aB and CRP are shown in Figure 3. The response was taken as the fractional change in I_{DS} after incubation with a given solution of protein compared to the I_{DS} in absence of that protein I_0 (response = $\Delta I/I_0 = (I_{DS} - I_0)/I_0$). Figure 3a shows how loading of SA to system A leads to an increase in the response while the AV binding reduces the response. At variance, further binding aB (Figure 3b) reduces the response and after CRP the response increases (Figure 3c), independently from the nature (SA or AV) of the protein in system B.

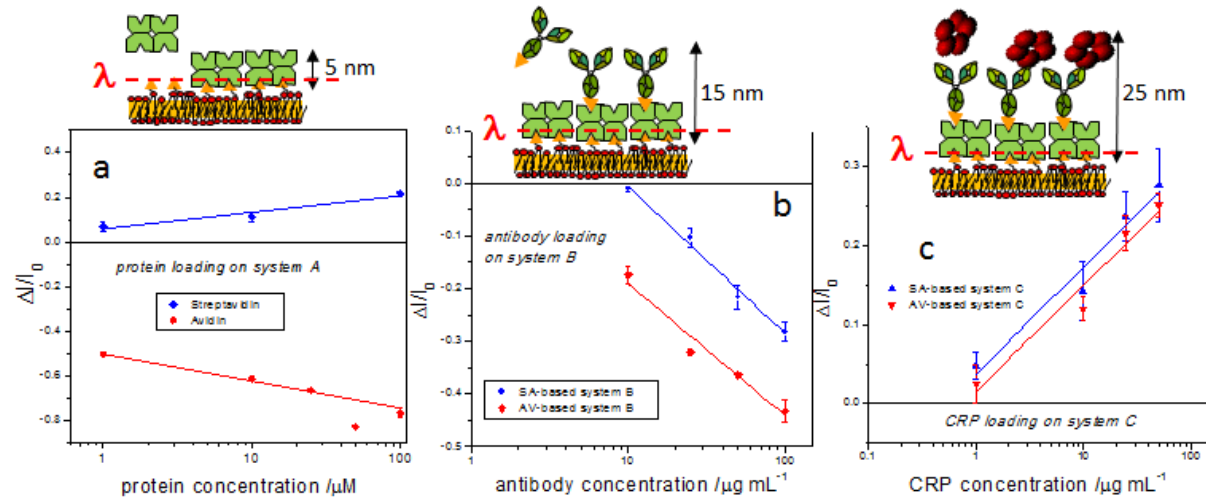


Figure 3. Relative response of the current versus the protein concentration for a) system A, b) system B, c) system C

To identify what modulates the device response, we estimated the relative changes of V_T and capacitance. The drain current in the saturation regime (*i.e.* $V_{DS} > (V_G - V_T)$) is given by:

$$I_{DS} = \frac{W}{2L} C \mu (V_G - V_T)^2 \quad (1)$$

where W and L are the width and the length of the channel. According to equation (1) V_T and the product μC can be evaluate by linear interpolation of the $\sqrt{I_{DS}}$ dependence on V_G and the response is given by:

$$\frac{\Delta I}{I_0} = \frac{\Delta C}{C_0} + \frac{2\Delta V_T}{(V_G - V_{T0})} \quad (2)$$

where the subscript 0 denotes the system chosen as reference. Assuming that μ is constant, the relative changes of V_T and C upon binding for the different systems are shown in Figure 4 for the highest concentration of proteins added.

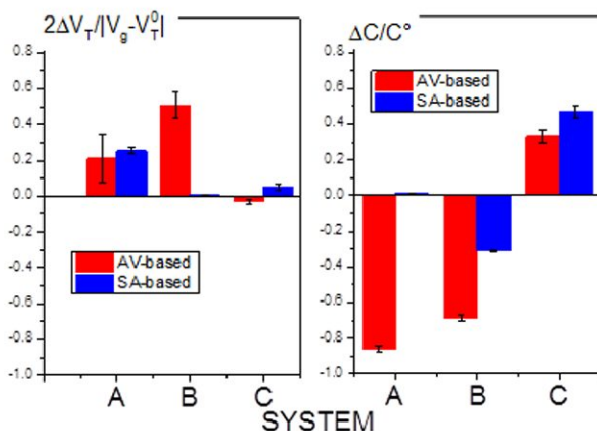


Figure 4. Relative changes of V_T and capacitance at the highest protein loading for all systems.

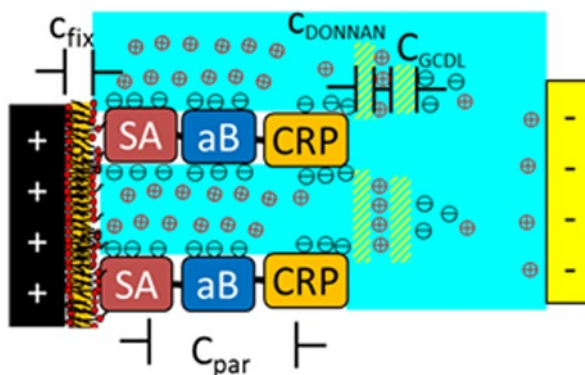


Figure 5. Schematic illustration of the capacitors contributing to the total gating capacitance

Comparison of these results with the $\Delta I/I_0$ at highest protein loading indicates that the response to the analyte (protein) is mainly capacitive. Although SA and AV hold opposite charges, their binding to system A give similar responses for V_T therefore the decrease of the current observed with AV is due to a 80% decrease in capacitance. In the case of systems B and D, one must consider the polyelectrolyte nature of proteins. The bound proteins are charged and the space between them is analogous to an ionic gel where the fixed polyelectrolyte ions establish a continuous background charge, and the mobile counter-ions can move freely within the layer. The counter-ions cannot diffuse too far into the solution because they form a net opposite charge in the protein layer leading to a Donnan's equilibrium. An electrical double layer is formed at the outer protein layer by the excess of counter-ions and the fixed charges as illustrated in Figure 5

The presence of the Donnan's equilibrium leads to the building-up of additional electrical potential and capacitance. Therefore the overall capacitance of the EG-TFT has a contribution from a series of capacitors: a fixed capacitance = C_{fix} accounting for the HDL and the PL bilayer capacitance, the GCDL ($C_{GCDL} \propto i_s^{1/2}$) and, in the presence of

protein layer, the Donnan's capacitance that is proportional to the ionic strength ($C_{DON} \propto i_s$). Possibly there are also some contributions to the capacitance that are in parallel and will be denoted by C_{par} . Therefore, the overall capacitance can be described as:

$$C = \left(\frac{1}{C_{fix}} + \frac{1}{C_{GCDL}} + \frac{1}{C_{DON}} \right)^{-1} + C_{par} \quad (3)$$

When only the PL bilayer is present $C = (C_{fix}^{-1} + C_{GCDL}^{-1})^{-1}$ but the protein binding adds with the C_{DONNAN} and C_{par} terms and this affects the device response. According to this model, the bio EG-TFT response is indeed governed by a capacitive effect that is independent from the position at which the Donnan's equilibrium is set and therefore does not depend on Debye's length. The latter dominates in electrostatic, rather than capacitive, detections

4. CONCLUSIONS

In summary, we studied a multilayer protein system coupled to an EG-TFT sensing platform. A bio EG-TFT sensing platform comprising a biological layer at the interface between the OS and the electrolyte was used. Although, TFTs are thought to be well suited for electronic detection that relies on electrostatic interactions with analyte biomolecules, herein, we demonstrated that sensing mechanism can be associated with capacitance changes. The mechanism of transduction has been ascribed to the formation of Donnan's equilibria within the protein layer, resulting in an extra capacitance in series to the gating system. This finding is important as it confirms the EG-TFT platform can be used for the detection of charged and neutral biomolecules. Moreover, detection is possible even if the value of Debye's length is below that of the distance at which the recognition event takes place.

ACKNOWLEDGMENT

Dr. Maria Magliulo is acknowledged for useful discussion. The "OrgBIO" Organic Bioelectronics (PITN-GA-2013-607896), the PON SISTEMA (MIUR) projects and CSGI are acknowledged for financial support

REFERENCES

- [1] Cramer, T., Campana, A., Leonardi, F., Casalini, S., Kyndiah, A., Murgia, M., and Biscarini, F., "Water-gated organic field effect transistors—opportunities for biochemical sensing and extracellular signal transduction," *J. Mater. Chem. B* 1(31), 3728-3741 (2013)
- [2] Torsi, L., Magliulo, M., Manoli, K., and Palazzo, G., "Organic field-effect transistor sensors: A tutorial review," *Chem. Soc. Rev.* 42(22), 8612-8628 (2013)
- [3] Marinelli, F., Dell'Aquila, A., Torsi, L., Tey, J., Suranna, G. P., Mastrorilli, P., Romanazzi, G., Nobile, C. F., Mhaisalkar, S. G., Cioffi, N., Palmisano, F., "An organic field effect transistor as a selective NO(x) sensor operated at room temperature," *Sens. Actuators B Chem.*, 140(12), 445-450 (2009)
- [4] Kergoat, L., Herlogsson, L., Braga, D., Piro, B., Pham, M.C., Crispin, X., Berggren, M., and Horowitz, G., "A Water-Gate Organic Field-Effect Transistor," *Adv. Mater.* 22(23), 2565-2569 (2010)
- [5] Kim, S.H., Hong, K., Xie, W., Lee, K.H., Zhang, S., Lodge, T.P., and Frisbie, C.D., "Electrolyte-Gated Transistors for Organic and Printed Electronics," *Adv. Mater.* 25(13), 1822-1846 (2013)
- [6] Magliulo, M., Mallardi, A., Mulla, M.Y., Cotrone, S., Pistillo, B.R., Favia, P., Vikholm-Lundin, I., Palazzo, G., and Torsi, L., "Electrolyte-Gated Organic Field-Effect Transistor Sensors Based on Supported Biotinylated Phospholipid Bilayer," *Adv. Mater.* 25(14), 2090-2094 (2013)
- [7] Buth, F., Donner, A., Sachsenhauser, M., Stutzmann, M., and Garrido, J.A., "Biofunctional Electrolyte-Gated Organic Field-Effect Transistors," *Adv. Mater.* 24(33), 4511-4517 (2012)
- [8] Cotrone, S., Ambrico, M., Toss, H., Angione, M.D., Magliulo, M., Mallardi, A., Berggren, M., Palazzo, G., Horowitz, G., and Ligonzo, T., "Phospholipid film in electrolyte-gated organic field-effect transistors," *Org. Electron.* 13(4), 638-644 (2012)
- [9] Kergoat, L., Piro, B., Berggren, M., Pham, M.-C., Yassar, A., and Horowitz, G., "DNA detection with a water-gated organic field-effect transistor," *Org. Electron.* 13(1), 1-6 (2012)

- [10] Vacic, A., Criscione, J.M., Rajan, N.K., Stern, E., Fahmy, T.M., and Reed, M.A., "Determination of molecular configuration by Debye length modulation," *J. Am. Chem. Soc.* 133(35), 13886-13889 (2011)
- [11] Stern, E., Wagner, R., Sigworth, F.J., Breaker, R., Fahmy, T.M., and Reed, M.A., "Importance of the Debye screening length on nanowire field effect transistor sensors," *Nano Lett.* 7(11), 3405-3409 (2007)
- [12] Palazzo, G., De Tullio, D., Magliulo, M., Mallardi, A., Intranuovo, F., Mulla, M.Y., Favia, P., Vikholm-Lundin, I., and Torsi, L., "Detection Beyond Debye's Length with an Electrolyte-Gated Organic Field-Effect Transistor," *Adv. Mater.* 27(5), 911-916 (2015)
- [13] Mulla, M.Y., Tuccori, E., Magliulo, M., Lattanzi, G., Palazzo, G., Persaud, K., and Torsi, L., "Capacitance-modulated transistor detects odorant binding protein chiral interactions," *Nat. Commun.* 6(6010), 1-9 (2015)
- [14] Suspène, C., Piro, B., Reisberg, S., Pham, M.-C., Toss, H., Berggren, M., Yassar, A., and Horowitz, G., "Copolythiophene-based water-gated organic field-effect transistors for biosensing," *J. Mater. Chem. B* 1(15), 2090-2097 (2013)
- [15] Manoli, K., Magliulo, M., Mulla, M.Y., Singh, M., Sabbatini, L., Palazzo, G., and Torsi, L., "Printable bioelectronics to investigate functional biological interfaces," *Angew. Chem. Int. Ed.* 54(43), 12562-12576 (2015)
- [16] Heller, I., Janssens, A.M., Männik, J., Minot, E.D., Lemay, S.G., and Dekker, C., "Identifying the mechanism of biosensing with carbon nanotube transistors," *Nano Lett.* 8(2), 591-595 (2008)
- [17] Urien, M., Wantz, G., Cloutet, E., Hirsch, L., Tardy, P., Vignau, L., Cramail, H., and Parneix, J.-P., "Field-effect transistors based on poly (3-hexylthiophene): Effect of impurities," *Org. Electron.* 8(6), 727-734 (2007)
- [18] Torsi, L., Dodabalapur, A., Lovinger, A. J., Katz, H. E., Ruel, R., Davis, D. D. and Baldwin, K. W., "Rapid thermal processing of α -hexathiophene thin-film transistors," *Chem. Mater.* 7(12), 2247-2251 (1995)
- [19] Lovinger, A. L., Davis, D. D., Dodabalapur, A., Katz, H. E., and Torsi L., "Single-Crystal and Polycrystalline Morphology of the Thiophene-Based Semiconductor α -Hexathiophene (α -6T)," *Macromolecules* 29(14), 4952-4957 (1996)
- [20] Magliulo, M., Pistillo, B.R., Mulla, M.Y., Cotrone, S., Ditaranto, N., Cioffi, N., Favia, P., and Torsi, L., "PE-CVD of Hydrophilic-COOH Functionalized Coatings on Electrolyte Gated Field-Effect Transistor Electronic Layers," *Plasma Process Polym.* 10(2), 102-109 (2013)
- [21] Kastellorizios, M., Michanetzis, G.P., Pistillo, B.R., Mourtas, S., Klepetsanis, P., Favia, P., Sardella, E., d'Agostino, R., Missirlis, Y.F., and Antimisariaris, S.G., "Haemocompatibility improvement of metallic surfaces by covalent immobilization of heparin-liposomes," *Int. J. Pharm.* 432(1), 91-98 (2012)
- [22] Pistillo, B.R., Perrotta, A., Gristina, R., Ceccone, G., Nardulli, M., d'Agostino, R., and Favia, P., "Water resistant ethylene/acrylic acid plasma-deposited coatings," *Surf. Coat. Technol.* 205, S534-S536 (2011)
- [23] Braga, D., and Horowitz, G., "High-Performance Organic Field-Effect Transistors," *Adv. Mater.* 21(14-15), 1473-1486 (2009)
- [24] Leckband, D., and Israelachvili, J., "Molecular basis of protein function as determined by direct force measurements," *Enzyme Microb. Technol.* 15(6), 450-459 (1993)
- [25] Diamandis, E.P., and Christopoulos, T.K., "The biotin-(strept) avidin system: principles and applications in biotechnology," *Clin. Chem.* 37(5), 625-636 (1991)
- [26] Osmand, A.P., Friedenson, B., Gewurz, H., Painter, R.H., Hofmann, T., and Shelton, E., "Characterization of C-reactive protein and the complement subcomponent C1t as homologous proteins displaying cyclic pentameric symmetry (pentraxins)," *Proc Natl Acad Sci U S A* 74(2), 739-743 (1977)